

1 **Appendix A. Balance equations**

2 We use a combined numerical strategy for modelling convection by solid-
 3 state creep in the Earth's mantle as well as partial melting in some of the
 4 upper regions of the mantle, processes that lead to the segregation and for-
 5 mation of the precursors of continental crustal material as well as mixing
 6 within the remaining mantle. We solve differential equations relating to
 7 infinite Prandtl-number convection using a three-dimensional finite-element
 8 spherical-shell method that ensures the conservation of mass, momentum,
 9 and energy. The mass balance

$$10 \quad \frac{\partial \rho}{\partial t} + \nabla \cdot (\rho \vec{v}) = 0 \quad (\text{A.1})$$

11 with an anelastic-liquid approximation simplifies to

$$12 \quad \nabla \cdot \vec{v} = -\frac{1}{\rho} \vec{v} \cdot \nabla \rho \quad (\text{A.2})$$

13 where ρ is density, t is time, and \vec{v} is velocity.

14 The conservation of momentum can be written as

$$15 \quad \rho \left(\frac{\partial \vec{v}}{\partial t} + \vec{v} \cdot \nabla \vec{v} \right) = -\nabla P + \rho \vec{g} + \frac{\partial}{\partial x_k} \tau_{ik} \quad (\text{A.3})$$

16 where P is pressure, \vec{g} is acceleration due to gravity, and τ_{ik} is the devia-
 17 toric stress tensor. Spherical symmetry is modelled using $\vec{g} = -g\vec{e}_r$ and the
 18 hydrostatic pressure gradient is defined as

$$19 \quad -\frac{\partial P}{\partial r} = \rho g \quad (\text{A.4})$$

20 By definition, $K_S = -V \left(\frac{\partial P}{\partial V} \right)_S$ and $\frac{V}{V_0} = \frac{\rho_0}{\rho}$, where K_S is the adiabatic bulk
 21 modulus, V is volume, S is entropy, and r is the radial distance from the
 22 Earth's centre. Hence,

$$23 \quad K_S = \rho \left(\frac{\partial P}{\partial \rho} \right)_S = \rho \left(\frac{\partial P}{\partial r} \right)_S \left(\frac{\partial r}{\partial \rho} \right)_S \quad (\text{A.5})$$

24 Substituting Eq. (A.4) into Eq. (A.5) yields

$$25 \quad \left(\frac{\partial \rho}{\partial r} \right)_S = \frac{-\rho^2 g}{K_S} \quad (\text{A.6})$$

26 If horizontal spatial variations in ρ are ignored, Eqs. (A.2) and (A.6)
 27 yield

$$28 \quad \nabla \cdot \vec{v} = -\frac{1}{\rho} \vec{v} \cdot \nabla \rho \cong -\frac{1}{\rho} v_r \frac{\partial \rho}{\partial r} = \frac{\rho g v_r}{K_S} \quad (\text{A.7})$$

29 It is well known that

$$30 \quad K_S = \frac{c_p}{c_v} K_T = (1 + \alpha \gamma_{th} T) K_T \quad (\text{A.8})$$

31 where K_T is the isothermal bulk modulus, c_p is specific heat at a constant
 32 pressure, c_v is specific heat at a constant volume, α is the coefficient of
 33 thermal expansion, γ_{th} is the thermodynamic Grüneisen parameter, and T is
 34 the absolute temperature.

35 This means that eq. (A.3) can be rewritten as

$$36 \quad \rho \frac{dv_i}{dt} = \rho g_i + \frac{\partial \sigma_{ki}}{\partial x_k} \quad (\text{A.9})$$

37 This in turn means that the energy balance can be expressed as follows

$$38 \quad \rho \frac{du}{dt} + \frac{\partial q_i}{\partial x_i} = Q + \sigma_{ik} \dot{\epsilon}_{ik} \quad (\text{A.10})$$

39 where u is specific internal energy, Q is heat generation rate per unit volume,
 40 and v_i , g_i , q_i , x_i , σ_{ik} , and $\dot{\epsilon}_{ik}$ are velocity, gravity acceleration, heat flow
 41 density, location vector, stress tensor, and strain-rate tensor components,
 42 respectively.

43 Another formulation of Eq. (A.10) is

$$44 \quad \rho \left[\frac{\partial}{\partial t} + \vec{v} \cdot \nabla \right] u = \nabla \cdot (k \nabla T) + Q - P \nabla \cdot \vec{v} + 2W_D \quad (\text{A.11})$$

45 where

$$46 \quad 2W_D = \sigma_{ik} \dot{\epsilon}_{ik} + P \nabla \cdot \vec{v} \quad (\text{A.12})$$

47 and

$$48 \quad q_k = -k \frac{\partial T}{\partial x_k} \quad (\text{A.13})$$

49 with k indicating thermal conductivity. Using

$$50 \quad du = T ds - P dv \quad (\text{A.14})$$

51 and

$$52 \quad du = T \left(\frac{\partial s}{\partial T} \right)_P dT + T \left(\frac{\partial s}{\partial P} \right)_T dP - Pdv \quad (\text{A.15})$$

53 eliminates specific internal energy (u) in Eq. (A.11), yielding the following
54 equation

$$55 \quad \rho c_p \frac{dT}{dt} = \nabla \cdot (k \nabla T) + Q + \alpha T \frac{dP}{dt} + 2W_D \quad (\text{A.16})$$

56 as

$$57 \quad c_p = T \left(\frac{\partial s}{\partial T} \right)_P \quad \text{and} \quad \left(\frac{\partial s}{\partial P} \right)_T = - \left(\frac{\partial v}{\partial T} \right)_P = -v\alpha \quad (\text{A.17})$$

58 where s represents specific entropy, v specific volume, c_p specific heat at a
59 constant pressure, and α the coefficient of thermal expansion.

60 A less well-known version of the energy balance can be deduced, as Eq.
61 (A.11) is equivalent to

$$62 \quad \rho \left(\frac{du}{dt} + P \frac{dv}{dt} \right) = \tau_{ik} \frac{\partial v_i}{\partial x_k} + \nabla \cdot (k \nabla T) + Q \quad (\text{A.18})$$

63 because of Eq. (A.2) and $\frac{1}{\rho} = v$.

64 Inserting Eq. (A.14) into Eq. (A.18) yields

$$65 \quad \rho T \frac{ds}{dt} = \tau_{ik} \frac{\partial v_i}{\partial x_k} + \frac{\partial}{\partial x_j} \left(k \frac{\partial}{\partial x_j} T \right) + Q \quad (\text{A.19})$$

66 However,

$$67 \quad ds = \left(\frac{\partial s}{\partial T} \right)_v dT + \left(\frac{\partial s}{\partial v} \right)_T dv \quad (\text{A.20})$$

68 and

$$69 \quad \left(\frac{\partial s}{\partial T}\right)_v = \frac{c_v}{T}, \quad \left(\frac{\partial s}{\partial v}\right)_T = \alpha K_T \quad (\text{A.21})$$

70 suggests that

$$71 \quad Tds = c_v dT + \alpha K_T T d\left(\frac{1}{\rho}\right) \quad (\text{A.22})$$

72 or

$$73 \quad Tds = c_v dT - \frac{c_v \gamma T}{\rho} d\rho \quad (\text{A.23})$$

74 where

$$75 \quad \gamma_{th} = \frac{\alpha K_T}{c_v \rho} \quad (\text{A.24})$$

76 indicates the thermodynamic Grüneisen parameter.

77 Inserting Eq. (A.23) into Eq. (A.19) yields

$$78 \quad \rho c_v \frac{dT}{dt} - c_v \gamma T \frac{d\rho}{dt} = \tau_{ik} \frac{\partial v_i}{\partial x_k} + \frac{\partial}{\partial x_j} \left(k \frac{\partial}{\partial x_j} T \right) + Q \quad (\text{A.25})$$

79 with Eqs. (A.1) and (A.25) yielding

$$80 \quad \rho c_v \frac{dT}{dt} = -\rho c_v \gamma T \frac{\partial v_j}{\partial x_j} + \tau_{ik} \frac{\partial v_i}{\partial x_k} + \frac{\partial}{\partial x_j} \left(k \frac{\partial}{\partial x_j} T \right) + Q \quad (\text{A.26})$$

81 or

$$82 \quad \frac{\partial T}{\partial t} = -v_j \frac{\partial}{\partial x_j} T - \gamma T \frac{\partial v_j}{\partial x_j} + \frac{1}{\rho c_v} \left[\tau_{ik} \frac{\partial v_i}{\partial x_k} + \frac{\partial}{\partial x_j} \left(k \frac{\partial}{\partial x_j} T \right) + Q \right] \quad (\text{A.27})$$

83 or

$$84 \quad \frac{\partial T}{\partial t} = -\frac{\partial(Tv_j)}{\partial x_j} - (\gamma - 1)T \frac{\partial v_j}{\partial x_j} + \frac{1}{\rho c_v} \left[\tau_{ik} \frac{\partial v_i}{\partial x_k} + \frac{\partial}{\partial x_j} \left(k \frac{\partial}{\partial x_j} T \right) + Q \right] \quad (\text{A.28})$$

85 This is an alternative formula for energy conservation. Although c_v appears
 86 in Eq. (A.28), the latter expression is equivalent to Eq. (A.16), which uses
 87 c_p . The deviatoric stress tensor can be expressed by

$$88 \quad \tau_{ik} = \eta \left(\frac{\partial v_i}{\partial x_k} + \frac{\partial v_k}{\partial x_i} - \frac{2}{3} \frac{\partial v_j}{\partial x_j} \delta_{ik} \right) \quad (\text{A.29})$$

89 in Eqs. (A.3) and (A.28), where η denotes viscosity.

90 As an *equation of state* we use

$$91 \quad \rho = \rho_r \left[1 - \alpha(T - T_r) + K_T^{-1}(P - P_r) + \sum_{k=1}^2 \Gamma_k \Delta \rho_k / \rho_r \right] \quad (\text{A.30})$$

92 where the index r refers to the adiabatic reference state, $\Delta \rho_k / \rho_r$ or f_{ak} de-
 93 notes the non-dimensional density jump for the k th mineral phase transi-
 94 tion, and Γ_k is a measure of the relative fraction of the heavier phase, where
 95 $\Gamma_k = \frac{1}{2} \left(1 + \tanh \frac{\pi_k}{d_k} \right)$ with $\pi_k = P - P_{0k} - \gamma_k T$ describing excess pressure π_k .
 96 The quantity P_{0k} is the transition pressure for the vanishing temperature T .
 97 A non-dimensional transition width is denoted by d_k , with γ_k representing
 98 the Clausius–Clapeyron slope for the k th phase transition. Γ_k and π_k were
 99 introduced by Richter (1973) and Christensen and Yuen (1985),
 100 with the presence of very high Prandtl numbers meaning that the left-hand
 101 side of Eq. (A.3) vanishes. As such, we use the following version of the
 102 equation of conservation of momentum:

$$103 \quad 0 = -\frac{\partial}{\partial x_i}(P - P_r) + (\rho - \rho_r)g_i(r) + \frac{\partial}{\partial x_k}\tau_{ik} \quad (\text{A.31})$$

104 The final version of the conservation of mass equation is

$$105 \quad 0 = \frac{\partial}{\partial x_j}\rho v_j, \quad (\text{A.32})$$

106 which stems from Eq. (A.2). Equations (A.28), (A.30), (A.31) and (A.32)
 107 are a system of six scalar equations that can be used to determine six scalar
 108 unknown functions, namely T , ρ , P , and the three components of v_i .

109 **Appendix B. Supplementary data**

110 Below, we specify the input parameters of our dynamic model. For the
 111 upper mantle, we use a peridotite solidus, T_{sol} , modified according to Litasov
 112 (2011). Cf. Fig. B1. T_{sol} is not only a function of pressure P but also
 113 of the water abundance which is a variable. We suppose that, inside the
 114 variable volume of chemical differentiation, the amount of water is diminished
 115 from 1000 ppm H₂O to zero during one differentiation event. Thereafter,
 116 the modelled rock continues to creep according the full system of partial
 117 differential equations, ensuring the conservation of mass, energy momentum,
 118 and angular momentum. The lower mantle solidus has been computed using

$$119 \quad \frac{1}{T_{sol}} \cdot \frac{dT_{sol}}{dP} = \frac{2}{K} \left(\gamma_{ax} - \frac{1}{3} \right) \quad (\text{B.1})$$

120 where T_{sol} is the solidus, P is pressure, and K is the bulk modulus according
 121 to PREM (Preliminary reference Earth model; cf. Dziewonski and Anderson,
 122 1981). For depth between 771 and 2741 km, we calculated the used Grüneisen
 123 parameter γ_{ax} using the acoustic gamma, γ_a :

$$\begin{aligned} \gamma_a = & \frac{1}{6} \frac{K_T}{K_S + (4/3)\mu} \left[\left(\frac{\partial K_S}{\partial P} \right)_T + \frac{4}{3} \left(\frac{\partial \mu}{\partial P} \right)_T \right] \\ & + \frac{1}{3} \frac{K_T}{\mu} \left(\frac{\partial \mu}{\partial P} \right)_T - \frac{1}{6} \end{aligned} \quad (\text{B.2})$$

124 It is remarkable that γ_a can be completely determined from geophysically
 125 observable variables obtained from PREM. This means that our model is
 126 independent of specific chemical or mineralogical models at these depths.
 127 K_T denotes the isothermal bulk modulus, K_S the adiabatic bulk modulus,
 128 μ the shear modulus. It would be straightforward to utilize Eqs. (B.1) and
 129 (B.2) also for upper mantle, crust, and D'' layer. However, we must pay
 130 attention to the observation by Stacey and Davis (2009) that seismological
 131 estimates of dK/dP and $d\mu/dP$ within upper mantle, crust, and D'' layer
 132 generate physically implausible depth variations of the Grüneisen parameter
 133 γ . That is why we use the gamma estimates of Stacey and Davis (2009), γ_{SD} ,
 134 for the depth range $h < 771$ km and for the D'' layer; otherwise, our model
 135 uses γ_a . We call this combination the extended acoustic gamma, γ_{ax} . To get
 136 a feeling whether our estimation of γ_a is reliable, we additionally compute

137 the Debye gamma, γ_D , using

$$138 \quad \gamma_D = \frac{1}{3} - \frac{1}{3} \left[d \ln \left(\frac{1}{v_p^3} + \frac{2}{v_s^3} \right) / d \ln \rho \right] \quad (\text{B.3})$$

139 where v_p and v_s indicate the seismic compressional and shear wave velocities,
 140 respectively. These velocities and the density, ρ , were taken from PREM.
 141 Fig. B2 shows a comparison of the three gamma functions the numerical
 142 values of which are given in Table B1. As well-known, the viscosity of the
 143 mantle is a crucial parameter for the thermal evolution of the Earth. The
 144 viscosity, η , has been computed using Eq. (7). The quantity η is nonlinearly
 145 dependent on the melting temperature, T_m , the dependence of which on the
 146 Grüneisen parameter by Eq. (B.1). The quantity $\eta_4(r)$, appearing in Eq. (7),
 147 is specified in Table B1. It bears a certain resemblance to the mantle viscosity
 148 deduced by Mitrovica and Forte (2004). To make our computations traceable,
 149 we add the adiabatic temperature T_{ad} (K), the thermal expansion coefficient
 150 α ($10^{-6} \cdot \text{K}^{-1}$) and the specific heat at constant pressure c_p (J/(kg · K)) as a
 151 function of depth h (km) to Table B1. The α/c_p ratio is determined by

$$152 \quad \alpha/c_p = (\gamma_{ax} \cdot \rho) / K_T \quad (\text{B.4})$$

$$153 \quad \text{where } K_T = (1 + \alpha \cdot \gamma_{ax} \cdot T)^{-1} \cdot K_s \quad (\text{B.5})$$

155 using PREM again. Further input parameters are presented by Table B2.

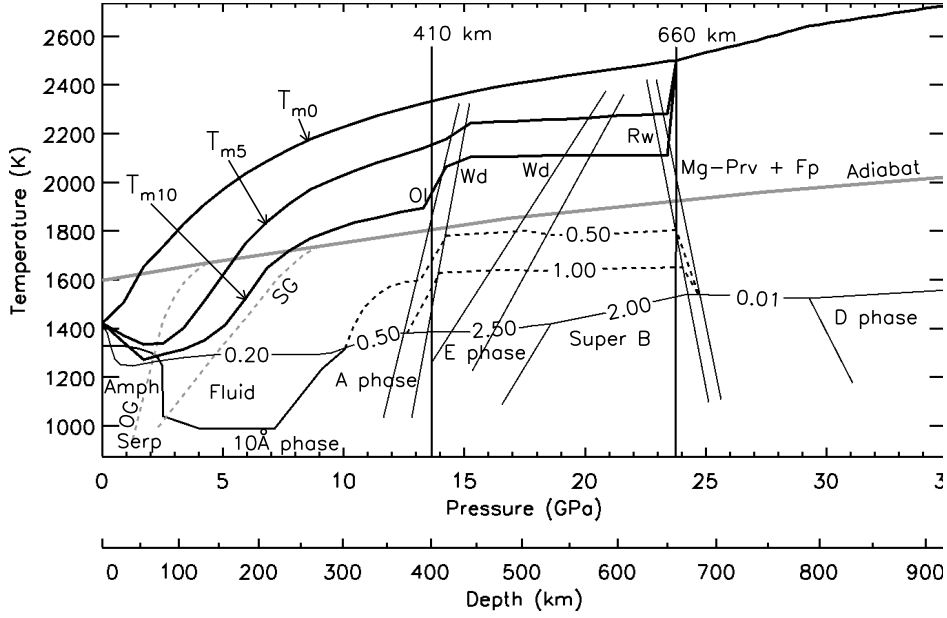


Fig. B1. Variations of peridotite solidi (T_{sol}) as a function of pressure (P) and water abundance, modified according to Litasov (2011). The curve for 0 ppm H_2O is denoted by T_{m0} , for 500 ppm H_2O by T_{m5} , and for 1000 ppm H_2O by T_{m10} . Ol = olivine, Wd = wadsleyite, Rw = ringwoodite, Mg-Prv = magnesium perovskite, Fp = ferropericlasite. The MORB adiabat at a potential temperature of 1588 K is labelled as *Adiabat*. MORB is the abbreviation for mid-oceanic ridge basalt.

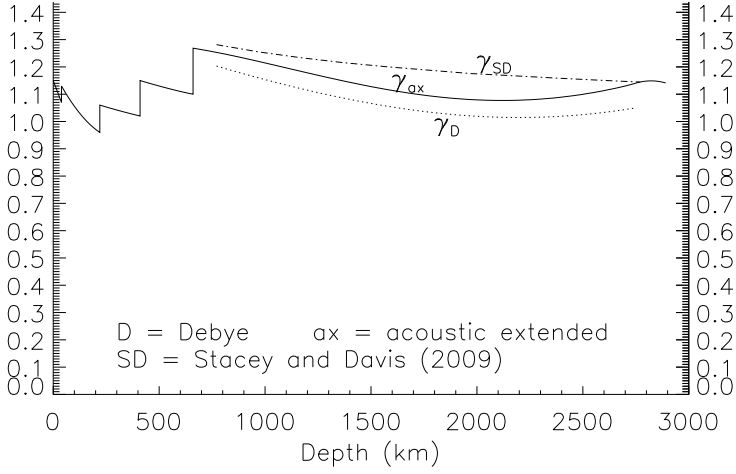


Fig. B2. Comparison of different Grüneisen parameters (γ) as a function of depth (h). The γ values according to Stacey and Davis (2009) are denoted by γ_{SD} . Our newly deduced extended acoustic gamma is referred to as γ_{ax} , and the Debye gamma as γ_D .

Table B1.

Physical properties of the mantle as a function of depth (h). The extended acoustic Grüneisen parameter (γ_{ax}) and Debye gamma (γ_D) values were determined using PREM observational values. The Grüneisen parameter of Stacey and Davis (2009) is indicated by γ_{SD} . The quantity T_{m0} denotes the dry peridotite solidus with T_{m5} and T_{m10} indicating the solidus of peridotite containing 500 ppm H₂O and 1000 ppm H₂O, respectively (Litasov, 2011). The viscosity level factor of Eq.(7) is indicated by η_4 , with T_{ad} indicating the adiabatic temperature of the mantle, α representing thermal expansivity, and c_p indicating specific heat values at a constant pressure. NaN means "Not a Number" as is customary in information technology.

(km)	Y_{ax}	Y_0	Y_{SD}	$T_{me}(K)$	$T_{ms}(K)$	$T_{m10}(K)$	$\log(\eta_a)$ (Pa·s)	$T_{ad}(K)$	α ($10^{-6}K^{-1}$)	cp (J/(kg·K))
0	1.1500	2.8689	-0.6467	1422.8	1422.8	1422.8	24.000	1601.2	40.000	695.2
10	1.1295	2.8701	-0.6485	1452.6	1404.7	1395.1	24.000	1605.2	43.333	766.8
20	1.1090	2.8714	-0.6496	1482.4	1386.6	1367.4	24.000	1609.2	46.667	1092.4
30	1.0885	2.8727	-0.9995	1516.2	1369.1	1339.7	24.000	1615.3	50.000	1785.0
39	1.0700	2.8738	-1.0013	1567.2	1356.1	1314.8	23.782	1624.6	53.000	1922.3
39	1.1300	2.8738	-1.0013	1567.2	1356.1	1314.8	23.782	1624.6	33.500	1150.5
40	1.1286	2.8739	-1.0015	1572.9	1354.7	1312.0	23.758	1625.1	33.477	1150.9
50	1.1153	2.8752	-1.0034	1629.5	1340.3	1284.3	23.516	1630.4	33.249	1155.1
60	1.1024	2.8765	-1.0052	1673.0	1334.9	1276.7	23.274	1637.4	33.027	1159.1
70	1.0900	2.8777	-1.0071	1705.8	1336.9	1285.1	23.032	1643.5	32.810	1162.9
80	1.0781	2.8790	-1.0089	1738.6	1338.9	1293.6	22.789	1648.2	32.598	1166.5
80	1.0781	2.8790	-1.0266	1738.6	1338.9	1293.6	22.789	1648.2	32.598	1166.5
90	1.0666	2.8803	-1.0265	1772.8	1361.9	1302.0	22.547	1653.0	32.392	1169.9
100	1.0556	2.8815	-1.0264	1807.1	1385.8	1310.5	22.305	1657.7	32.191	1173.0
110	1.0451	2.8828	-1.0264	1840.0	1416.6	1320.7	22.063	1662.4	31.996	1176.0
120	1.0350	2.8841	-1.0264	1870.3	1459.4	1334.2	21.821	1667.0	31.806	1178.6
130	1.0254	2.8854	-1.0264	1900.6	1502.1	1347.6	21.579	1671.9	31.621	1181.0
140	1.0163	2.8866	-1.0265	1928.2	1547.2	1369.1	21.337	1676.3	31.441	1183.2
150	1.0076	2.8879	-1.0266	1955.1	1592.9	1392.9	21.095	1680.2	31.267	1185.0
160	0.9994	2.8892	-1.0267	1981.1	1638.7	1420.3	20.853	1684.3	31.099	1186.6
170	0.9917	2.8905	-1.0269	2003.5	1684.9	1463.0	20.611	1688.6	30.936	1187.8
180	0.9844	2.8918	-1.0271	2025.8	1731.2	1505.7	20.368	1692.9	30.778	1188.7
190	0.9776	2.8931	-1.0274	2047.0	1770.4	1551.7	20.126	1697.4	30.625	1189.3
200	0.9713	2.8944	-1.0277	2067.4	1804.7	1599.9	19.884	1701.6	30.478	1189.6
210	0.9654	2.8957	-1.0280	2087.8	1839.0	1648.2	19.642	1705.4	30.336	1189.5
220	0.9600	2.8970	-1.0284	2106.2	1867.3	1676.1	19.400	1708.8	30.200	1189.1
220	1.0600	1.2321	1.0323	2106.2	1867.3	1676.1	19.400	1708.8	28.800	1209.1
230	1.0577	1.2322	1.0346	2124.6	1895.7	1703.9	19.432	1712.7	28.584	1209.2
240	1.0554	1.2322	1.0368	2142.0	1921.6	1728.3	19.463	1717.1	28.370	1209.3
250	1.0531	1.2323	1.0391	2157.9	1944.0	1747.7	19.495	1721.1	28.156	1209.3
260	1.0509	1.2324	1.0413	2173.8	1966.3	1767.1	19.526	1724.8	27.944	1209.3
270	1.0487	1.2325	1.0436	2188.1	1983.1	1781.3	19.558	1729.5	27.733	1209.2
280	1.0465	1.2325	1.0459	2202.0	1998.5	1794.2	19.589	1734.1	27.523	1209.0
290	1.0443	1.2326	1.0482	2215.5	2013.5	1806.8	19.621	1738.6	27.314	1208.8
300	1.0421	1.2327	1.0504	2227.4	2027.5	1818.2	19.653	1742.8	27.106	1208.5
310	1.0400	1.2328	1.0527	2239.3	2041.4	1829.6	19.684	1746.4	26.900	1208.2
320	1.0379	1.2328	1.0550	2251.0	2054.7	1838.9	19.716	1750.3	26.695	1207.8
330	1.0358	1.2329	1.0573	2262.4	2067.6	1846.9	19.747	1754.4	26.491	1207.3
340	1.0338	1.2330	1.0596	2273.8	2080.5	1854.8	19.779	1758.1	26.288	1206.8
350	1.0317	1.2331	1.0618	2284.2	2092.4	1863.3	19.811	1762.0	26.086	1206.2
360	1.0297	1.2331	1.0641	2294.7	2104.4	1871.7	19.842	1766.1	25.885	1205.6
370	1.0277	1.2332	1.0664	2304.5	2115.8	1879.3	19.874	1770.0	25.686	1204.9
380	1.0258	1.2333	1.0687	2313.4	2126.8	1885.8	19.905	1773.7	25.488	1204.2
390	1.0238	1.2334	1.0710	2322.3	2137.7	1892.2	19.937	1777.5	25.291	1203.4
400	1.0219	1.2334	1.0733	2331.3	2151.6	1949.1	19.968	1781.3	25.095	1202.5
410	1.0200	1.2335	1.0756	2340.2	2166.0	2015.2	20.000	1798.1	24.900	1201.6
410	1.1500	2.0697	3.2953	2340.2	2166.0	2015.2	20.000	1798.1	27.400	1228.0
420	1.1477	2.0654	3.3185	2349.1	2183.2	2068.4	20.684	1821.0	26.997	1225.5
430	1.1454	2.0612	3.3416	2357.5	2208.5	2083.3	21.368	1830.1	26.603	1223.0
440	1.1431	2.0570	3.3647	2366.0	2233.9	2098.2	22.052	1833.8	26.218	1220.6
450	1.1409	2.0528	3.3877	2374.1	2243.8	2103.7	22.736	1837.4	25.842	1218.3
460	1.1387	2.0487	3.4107	2382.0	2245.8	2104.2	22.736	1840.6	25.475	1216.0
470	1.1365	2.0447	3.4336	2389.9	2247.8	2104.7	22.736	1843.7	25.118	1213.9
480	1.1343	2.0406	3.4565	2396.4	2249.3	2105.2	22.736	1846.6	24.770	1211.9
490	1.1321	2.0367	3.4793	2402.8	2250.8	2105.6	22.736	1850.0	24.430	1210.0
500	1.1300	2.0328	3.5021	2409.0	2252.3	2106.4	22.736	1854.2	24.100	1208.3
510	1.1279	2.0289	3.5248	2415.0	2253.8	2107.4	22.736	1858.1	23.779	1206.7
520	1.1258	2.0250	3.5474	2421.0	2255.2	2108.4	22.736	1862.4	23.467	1205.3
520	1.1258	2.0250	3.5474	2421.0	2255.2	2108.4	22.736	1862.4	23.467	1205.3
530	1.1238	2.0213	3.5700	2426.9	2257.2	2108.9	22.736	1871.3	23.164	1204.0
540	1.1217	2.0175	3.5926	2432.9	2259.2	2109.4	22.736	1881.1	22.871	1203.0
550	1.1197	2.0138	3.6151	2438.9	2261.1	2109.8	22.736	1892.0	22.586	1202.1
560	1.1177	2.0101	3.6376	2444.8	2263.1	2109.8	22.736	1903.1	22.310	1201.5
570	1.1158	2.0065	3.6600	2450.8	2265.1	2109.8	22.736	1905.2	22.044	1201.1

h (km)	γ_{ax}	γ_0	γ_{SD}	$T_{ms}(K)$	$T_{ms}(K)$	$T_{m10}(K)$	$\log(\eta_a)$ (Pa·s)	$T_{ad}(K)$	α ($10^{-6}K^{-1}$)	cp (J/(kg·K))
580	1.1138	2.0029	3.6824	2456.5	2267.8	2109.8	22.736	1906.8	21.787	1201.0
590	1.1119	1.9994	3.7047	2462.1	2270.8	2109.8	22.736	1907.6	21.539	1201.1
600	1.1100	1.9958	3.7270	2467.6	2273.6	2109.8	22.736	1909.3	21.300	1201.5
600	1.1100	2.7450	0.6063	2467.6	2273.6	2109.8	22.736	1909.3	21.300	1201.5
610	1.1082	2.7430	0.6054	2473.2	2275.1	2109.8	22.280	1911.5	21.132	1197.7
620	1.1065	2.7410	0.6044	2478.8	2276.6	2109.8	21.824	1914.1	20.985	1195.1
630	1.1048	2.7390	0.6035	2484.4	2278.1	2109.8	21.368	1916.3	20.858	1193.5
640	1.1032	2.7370	0.6025	2489.9	2279.6	2109.8	20.912	1918.0	20.752	1192.9
650	1.1016	2.7350	0.6016	2495.5	2281.1	2109.8	20.456	1920.8	20.666	1193.5
660	1.1000	2.7331	0.6007	2501.1	2501.1	2501.1	20.000	1918.7	20.600	1195.2
660	1.2686	3.6735	0.9591	2501.1	NaN	NaN	20.000	1918.7	23.007	1237.9
670	1.2673	3.6691	0.9574	2510.6	NaN	NaN	20.000	1884.9	22.894	1236.8
680	1.2660	3.6646	0.9557	2522.7	NaN	NaN	20.000	1888.5	22.782	1235.7
690	1.2647	3.6602	0.9541	2533.8	NaN	NaN	20.000	1897.9	22.671	1234.7
700	1.2633	3.6558	0.9524	2543.5	NaN	NaN	20.000	1906.6	22.562	1233.7
710	1.2620	3.6515	0.9508	2553.0	NaN	NaN	20.000	1914.3	22.452	1232.7
720	1.2606	3.6472	0.9491	2563.2	NaN	NaN	20.000	1922.1	22.344	1231.7
730	1.2592	3.6430	0.9473	2572.5	NaN	NaN	20.000	1927.5	22.237	1230.8
740	1.2577	3.6388	0.9456	2583.4	NaN	NaN	20.000	1930.4	22.130	1229.8
750	1.2563	3.6346	0.9438	2595.6	NaN	NaN	20.000	1933.7	22.024	1228.9
760	1.2548	3.6305	0.9420	2605.7	NaN	NaN	20.019	1937.5	21.920	1228.1
770	1.2533	3.6264	0.9402	2618.8	NaN	NaN	20.091	1941.3	21.816	1227.2
771	1.2531	3.6260	0.9400	2620.0	NaN	NaN	20.099	1941.7	21.805	1227.1
771	1.2531	1.2031	1.4099	2620.0	NaN	NaN	20.099	1941.7	21.805	1227.1
780	1.2518	1.2010	1.4072	2628.9	NaN	NaN	20.162	1945.4	21.712	1227.7
790	1.2503	1.1988	1.4043	2641.0	NaN	NaN	20.232	1948.4	21.610	1228.4
800	1.2487	1.1965	1.4014	2647.8	NaN	NaN	20.300	1950.5	21.509	1229.0
810	1.2471	1.1943	1.3984	2654.6	NaN	NaN	20.367	1953.9	21.408	1229.7
820	1.2455	1.1921	1.3954	2661.3	NaN	NaN	20.432	1957.3	21.308	1230.4
830	1.2439	1.1898	1.3924	2668.1	NaN	NaN	20.496	1960.7	21.209	1231.0
840	1.2423	1.1876	1.3893	2674.8	NaN	NaN	20.559	1964.0	21.111	1231.7
850	1.2406	1.1854	1.3862	2681.4	NaN	NaN	20.621	1967.4	21.014	1232.4
860	1.2390	1.1832	1.3832	2688.1	NaN	NaN	20.681	1970.7	20.917	1233.1
870	1.2373	1.1810	1.3801	2694.8	NaN	NaN	20.740	1974.1	20.821	1233.8
871	1.2371	1.1808	1.3798	2695.4	NaN	NaN	20.746	1974.4	20.812	1233.9
880	1.2356	1.1789	1.3770	2701.4	NaN	NaN	20.798	1977.4	20.726	1234.5
890	1.2339	1.1767	1.3738	2708.0	NaN	NaN	20.855	1980.7	20.632	1235.2
900	1.2322	1.1745	1.3707	2714.6	NaN	NaN	20.910	1984.0	20.539	1235.9
910	1.2304	1.1724	1.3676	2721.1	NaN	NaN	20.964	1987.3	20.446	1236.7
920	1.2287	1.1703	1.3644	2727.6	NaN	NaN	21.018	1990.5	20.354	1237.4
930	1.2270	1.1681	1.3613	2734.1	NaN	NaN	21.070	1993.8	20.263	1238.1
940	1.2252	1.1660	1.3581	2740.6	NaN	NaN	21.121	1997.1	20.173	1238.8
950	1.2235	1.1639	1.3550	2747.1	NaN	NaN	21.171	2000.3	20.084	1239.5
960	1.2217	1.1618	1.3518	2753.5	NaN	NaN	21.219	2003.5	19.995	1240.3
970	1.2199	1.1597	1.3487	2760.0	NaN	NaN	21.267	2006.7	19.907	1241.0
971	1.2197	1.1595	1.3483	2760.6	NaN	NaN	21.272	2007.1	19.898	1241.1
980	1.2181	1.1576	1.3455	2766.4	NaN	NaN	21.314	2009.9	19.819	1241.7
990	1.2163	1.1556	1.3423	2772.8	NaN	NaN	21.360	2013.1	19.733	1242.5
1000	1.2146	1.1535	1.3391	2779.1	NaN	NaN	21.405	2016.3	19.647	1243.2
1010	1.2127	1.1515	1.3360	2785.4	NaN	NaN	21.449	2019.5	19.562	1243.9
1020	1.2109	1.1494	1.3328	2791.8	NaN	NaN	21.492	2022.6	19.478	1244.7
1030	1.2091	1.1474	1.3296	2798.1	NaN	NaN	21.534	2025.8	19.394	1245.4
1040	1.2073	1.1454	1.3265	2804.3	NaN	NaN	21.575	2028.9	19.311	1246.2
1050	1.2055	1.1434	1.3233	2810.6	NaN	NaN	21.615	2032.0	19.229	1246.9
1060	1.2037	1.1414	1.3201	2816.8	NaN	NaN	21.654	2035.2	19.148	1247.7
1070	1.2019	1.1394	1.3170	2823.0	NaN	NaN	21.693	2038.2	19.067	1248.5
1071	1.2017	1.1392	1.3167	2823.7	NaN	NaN	21.697	2038.6	19.059	1248.5
1080	1.2000	1.1374	1.3138	2829.2	NaN	NaN	21.730	2041.3	18.987	1249.2
1090	1.1982	1.1355	1.3107	2835.4	NaN	NaN	21.767	2044.4	18.908	1250.0
1100	1.1964	1.1335	1.3076	2841.6	NaN	NaN	21.803	2047.5	18.829	1250.8
1110	1.1945	1.1316	1.3044	2847.7	NaN	NaN	21.839	2050.6	18.751	1251.5
1120	1.1927	1.1297	1.3013	2853.8	NaN	NaN	21.873	2053.6	18.674	1252.3
1130	1.1909	1.1278	1.2982	2859.9	NaN	NaN	21.907	2056.7	18.597	1253.1
1140	1.1891	1.1259	1.2951	2866.0	NaN	NaN	21.940	2059.7	18.521	1253.8

h (km)	γ_{ax}	γ_0	γ_{SD}	$T_{ms}(K)$	$T_{ms}(K)$	$T_{m10}(K)$	$\log(\eta_*)$ (Pa·s)	$T_{ad}(K)$	α ($10^{-6}K^{-1}$)	cp (J/(kg·K))
1150	1.1873	1.1240	1.2920	2872.0	NaN	NaN	21.972	2062.7	18.446	1254.6
1160	1.1854	1.1221	1.2890	2878.0	NaN	NaN	22.003	2065.7	18.371	1255.3
1170	1.1836	1.1202	1.2859	2884.1	NaN	NaN	22.034	2068.7	18.297	1256.1
1171	1.1834	1.1200	1.2856	2884.6	NaN	NaN	22.037	2069.0	18.290	1256.2
1180	1.1818	1.1184	1.2829	2890.0	NaN	NaN	22.064	2071.7	18.224	1256.9
1190	1.1800	1.1165	1.2798	2896.0	NaN	NaN	22.093	2074.7	18.151	1257.6
1200	1.1782	1.1147	1.2768	2902.0	NaN	NaN	22.122	2077.7	18.079	1258.4
1210	1.1764	1.1129	1.2738	2907.9	NaN	NaN	22.150	2080.6	18.008	1259.2
1220	1.1746	1.1111	1.2708	2913.8	NaN	NaN	22.178	2083.6	17.937	1259.9
1230	1.1728	1.1093	1.2679	2919.7	NaN	NaN	22.205	2086.5	17.867	1260.7
1240	1.1710	1.1075	1.2649	2925.6	NaN	NaN	22.231	2089.5	17.798	1261.5
1250	1.1692	1.1058	1.2620	2931.4	NaN	NaN	22.256	2092.4	17.729	1262.3
1260	1.1675	1.1040	1.2591	2937.3	NaN	NaN	22.281	2095.3	17.661	1263.0
1270	1.1657	1.1023	1.2562	2943.1	NaN	NaN	22.306	2098.2	17.593	1263.8
1271	1.1655	1.1021	1.2559	2943.7	NaN	NaN	22.308	2098.5	17.586	1263.9
1280	1.1639	1.1005	1.2533	2948.9	NaN	NaN	22.330	2101.1	17.526	1264.6
1290	1.1622	1.0988	1.2504	2954.7	NaN	NaN	22.353	2104.0	17.459	1265.3
1300	1.1604	1.0971	1.2476	2960.5	NaN	NaN	22.376	2106.9	17.394	1266.1
1310	1.1587	1.0955	1.2448	2966.2	NaN	NaN	22.398	2109.8	17.328	1266.9
1320	1.1570	1.0938	1.2420	2971.9	NaN	NaN	22.420	2112.6	17.264	1267.6
1330	1.1553	1.0921	1.2392	2977.7	NaN	NaN	22.441	2115.5	17.200	1268.4
1340	1.1536	1.0905	1.2365	2983.4	NaN	NaN	22.462	2118.3	17.136	1269.1
1350	1.1519	1.0889	1.2338	2989.0	NaN	NaN	22.482	2121.1	17.073	1269.9
1360	1.1502	1.0872	1.2311	2994.7	NaN	NaN	22.502	2124.0	17.011	1270.6
1370	1.1485	1.0856	1.2284	3000.4	NaN	NaN	22.521	2126.8	16.949	1271.4
1371	1.1483	1.0855	1.2282	3000.9	NaN	NaN	22.523	2127.1	16.943	1271.5
1380	1.1468	1.0841	1.2258	3006.0	NaN	NaN	22.540	2129.6	16.888	1272.1
1390	1.1452	1.0825	1.2232	3011.6	NaN	NaN	22.558	2132.4	16.827	1272.8
1400	1.1436	1.0809	1.2206	3017.2	NaN	NaN	22.576	2135.2	16.767	1273.6
1410	1.1419	1.0794	1.2181	3022.8	NaN	NaN	22.593	2138.0	16.707	1274.3
1420	1.1403	1.0779	1.2156	3028.3	NaN	NaN	22.610	2140.8	16.648	1275.0
1430	1.1387	1.0764	1.2131	3033.9	NaN	NaN	22.627	2143.5	16.589	1275.7
1440	1.1371	1.0749	1.2106	3039.4	NaN	NaN	22.643	2146.3	16.531	1276.5
1450	1.1355	1.0734	1.2082	3044.9	NaN	NaN	22.659	2149.1	16.474	1277.2
1460	1.1340	1.0719	1.2058	3050.4	NaN	NaN	22.674	2151.8	16.417	1277.9
1470	1.1324	1.0705	1.2034	3055.9	NaN	NaN	22.690	2154.5	16.360	1278.6
1471	1.1323	1.0703	1.2032	3056.5	NaN	NaN	22.691	2154.8	16.355	1278.6
1480	1.1309	1.0690	1.2011	3061.4	NaN	NaN	22.704	2157.3	16.304	1279.3
1490	1.1294	1.0676	1.1988	3066.8	NaN	NaN	22.718	2160.0	16.249	1279.9
1500	1.1279	1.0662	1.1965	3072.3	NaN	NaN	22.732	2162.7	16.194	1280.6
1510	1.1264	1.0648	1.1943	3077.7	NaN	NaN	22.746	2165.4	16.139	1281.3
1520	1.1250	1.0635	1.1921	3083.1	NaN	NaN	22.759	2168.1	16.086	1281.9
1530	1.1235	1.0621	1.1899	3088.5	NaN	NaN	22.772	2170.8	16.032	1282.6
1540	1.1221	1.0608	1.1878	3093.9	NaN	NaN	22.784	2173.5	15.979	1283.2
1550	1.1206	1.0595	1.1857	3099.3	NaN	NaN	22.797	2176.2	15.926	1283.9
1560	1.1192	1.0582	1.1836	3104.6	NaN	NaN	22.808	2178.9	15.874	1284.5
1570	1.1178	1.0569	1.1816	3110.0	NaN	NaN	22.820	2181.6	15.823	1285.1
1571	1.1177	1.0567	1.1814	3110.5	NaN	NaN	22.821	2181.8	15.818	1285.2
1580	1.1165	1.0556	1.1796	3115.3	NaN	NaN	22.831	2184.2	15.771	1285.7
1590	1.1151	1.0543	1.1777	3120.6	NaN	NaN	22.842	2186.9	15.721	1286.3
1600	1.1138	1.0531	1.1758	3125.9	NaN	NaN	22.853	2189.5	15.671	1286.9
1610	1.1125	1.0519	1.1740	3131.2	NaN	NaN	22.863	2192.2	15.621	1287.4
1620	1.1113	1.0507	1.1722	3136.5	NaN	NaN	22.873	2194.8	15.571	1288.0
1630	1.1100	1.0495	1.1704	3141.8	NaN	NaN	22.882	2197.4	15.523	1288.6
1640	1.1087	1.0484	1.1686	3147.0	NaN	NaN	22.892	2200.1	15.474	1289.1
1650	1.1075	1.0472	1.1669	3152.2	NaN	NaN	22.901	2202.7	15.426	1289.7
1660	1.1063	1.0461	1.1653	3157.5	NaN	NaN	22.909	2205.3	15.378	1290.2
1670	1.1051	1.0450	1.1636	3162.7	NaN	NaN	22.918	2207.9	15.331	1290.7
1671	1.1050	1.0449	1.1635	3163.2	NaN	NaN	22.919	2208.2	15.326	1290.7
1680	1.1039	1.0439	1.1621	3167.9	NaN	NaN	22.926	2210.5	15.284	1291.2
1690	1.1028	1.0428	1.1606	3173.1	NaN	NaN	22.934	2213.1	15.238	1291.6
1700	1.1017	1.0417	1.1591	3178.3	NaN	NaN	22.941	2215.7	15.192	1292.1
1710	1.1006	1.0407	1.1577	3183.5	NaN	NaN	22.949	2218.3	15.146	1292.5
1720	1.0995	1.0397	1.1563	3188.6	NaN	NaN	22.956	2220.9	15.101	1292.9

h (km)	Y_{ax}	Y_D	Y_{SD}	T_{m0} (K)	T_{m5} (K)	T_{m10} (K)	$\log(\eta_a)$ (Pa·s)	T_{ad} (K)	α ($10^{-6}K^{-1}$)	cp (J/(kg·K))
1730	1.0984	1.0387	1.1549	3193.8	NaN	NaN	22.962	2223.4	15.056	1293.4
1740	1.0974	1.0377	1.1536	3198.9	NaN	NaN	22.969	2226.0	15.012	1293.8
1750	1.0964	1.0367	1.1523	3204.1	NaN	NaN	22.975	2228.6	14.967	1294.2
1760	1.0954	1.0358	1.1511	3209.2	NaN	NaN	22.981	2231.1	14.924	1294.6
1770	1.0944	1.0349	1.1499	3214.3	NaN	NaN	22.986	2233.7	14.880	1294.9
1771	1.0943	1.0348	1.1498	3214.8	NaN	NaN	22.987	2233.9	14.876	1295.0
1780	1.0935	1.0340	1.1488	3219.4	NaN	NaN	22.992	2236.2	14.837	1295.3
1790	1.0926	1.0331	1.1478	3224.5	NaN	NaN	22.997	2238.8	14.795	1295.6
1800	1.0917	1.0322	1.1468	3229.6	NaN	NaN	23.002	2241.3	14.752	1295.9
1810	1.0908	1.0314	1.1458	3234.7	NaN	NaN	23.006	2243.9	14.711	1296.1
1820	1.0900	1.0305	1.1449	3239.7	NaN	NaN	23.010	2246.4	14.669	1296.3
1830	1.0892	1.0297	1.1440	3244.8	NaN	NaN	23.014	2248.9	14.628	1296.6
1840	1.0884	1.0290	1.1432	3249.8	NaN	NaN	23.018	2251.4	14.587	1296.9
1850	1.0876	1.0282	1.1424	3254.9	NaN	NaN	23.021	2254.0	14.546	1297.1
1860	1.0868	1.0274	1.1416	3259.9	NaN	NaN	23.024	2256.5	14.506	1297.3
1870	1.0861	1.0267	1.1409	3264.9	NaN	NaN	23.027	2259.0	14.466	1297.5
1871	1.0860	1.0266	1.1409	3265.5	NaN	NaN	23.027	2259.2	14.462	1297.5
1880	1.0854	1.0260	1.1403	3270.0	NaN	NaN	23.030	2261.5	14.427	1297.6
1890	1.0848	1.0253	1.1398	3275.0	NaN	NaN	23.032	2264.0	14.387	1297.7
1900	1.0841	1.0247	1.1393	3280.0	NaN	NaN	23.034	2266.5	14.348	1297.8
1910	1.0835	1.0240	1.1388	3285.0	NaN	NaN	23.035	2269.0	14.309	1297.8
1920	1.0830	1.0234	1.1385	3290.0	NaN	NaN	23.037	2271.5	14.271	1297.9
1930	1.0824	1.0228	1.1381	3295.0	NaN	NaN	23.037	2274.0	14.233	1297.9
1940	1.0818	1.0222	1.1377	3300.0	NaN	NaN	23.038	2276.5	14.195	1298.0
1950	1.0813	1.0216	1.1374	3305.0	NaN	NaN	23.039	2278.9	14.158	1298.0
1960	1.0808	1.0211	1.1372	3309.9	NaN	NaN	23.039	2281.4	14.120	1298.0
1970	1.0804	1.0206	1.1370	3314.9	NaN	NaN	23.038	2283.9	14.083	1297.9
1971	1.0803	1.0205	1.1370	3315.4	NaN	NaN	23.038	2284.1	14.080	1297.9
1980	1.0800	1.0201	1.1369	3319.9	NaN	NaN	23.038	2286.4	14.047	1297.8
1990	1.0796	1.0196	1.1369	3324.8	NaN	NaN	23.037	2288.9	14.010	1297.7
2000	1.0792	1.0192	1.1370	3329.8	NaN	NaN	23.035	2291.3	13.974	1297.5
2010	1.0789	1.0187	1.1371	3334.7	NaN	NaN	23.034	2293.8	13.938	1297.3
2020	1.0787	1.0183	1.1373	3339.7	NaN	NaN	23.032	2296.2	13.902	1297.1
2030	1.0784	1.0179	1.1374	3344.6	NaN	NaN	23.030	2298.7	13.867	1296.9
2040	1.0781	1.0175	1.1376	3349.6	NaN	NaN	23.027	2301.2	13.832	1296.7
2050	1.0778	1.0172	1.1378	3354.5	NaN	NaN	23.024	2303.6	13.797	1296.5
2060	1.0776	1.0169	1.1381	3359.4	NaN	NaN	23.020	2306.1	13.762	1296.2
2070	1.0774	1.0166	1.1385	3364.4	NaN	NaN	23.017	2308.5	13.727	1295.9
2071	1.0774	1.0165	1.1386	3364.9	NaN	NaN	23.016	2308.8	13.724	1295.9
2080	1.0773	1.0163	1.1390	3369.3	NaN	NaN	23.012	2311.0	13.693	1295.5
2090	1.0772	1.0160	1.1395	3374.2	NaN	NaN	23.008	2313.4	13.659	1295.1
2100	1.0772	1.0158	1.1401	3379.1	NaN	NaN	23.003	2315.9	13.625	1294.7
2110	1.0772	1.0156	1.1408	3384.1	NaN	NaN	22.998	2318.3	13.591	1294.2
2120	1.0772	1.0154	1.1416	3389.0	NaN	NaN	22.992	2320.7	13.558	1293.7
2130	1.0772	1.0152	1.1422	3393.9	NaN	NaN	22.986	2323.2	13.524	1293.2
2140	1.0772	1.0151	1.1430	3398.8	NaN	NaN	22.979	2325.6	13.491	1292.8
2150	1.0772	1.0149	1.1438	3403.7	NaN	NaN	22.972	2328.1	13.458	1292.2
2160	1.0773	1.0148	1.1447	3408.6	NaN	NaN	22.964	2330.5	13.426	1291.7
2170	1.0774	1.0148	1.1457	3413.6	NaN	NaN	22.956	2332.9	13.393	1291.0
2171	1.0774	1.0148	1.1458	3414.1	NaN	NaN	22.955	2333.2	13.390	1291.0
2180	1.0776	1.0147	1.1467	3418.5	NaN	NaN	22.948	2335.4	13.361	1290.4
2190	1.0778	1.0147	1.1478	3423.4	NaN	NaN	22.939	2337.8	13.328	1289.7
2200	1.0781	1.0147	1.1490	3428.3	NaN	NaN	22.929	2340.2	13.296	1288.9
2210	1.0784	1.0147	1.1503	3433.2	NaN	NaN	22.919	2342.6	13.264	1288.1
2220	1.0787	1.0147	1.1516	3438.2	NaN	NaN	22.909	2345.1	13.233	1287.3
2230	1.0790	1.0148	1.1529	3443.1	NaN	NaN	22.898	2347.5	13.201	1286.5
2240	1.0793	1.0148	1.1542	3448.0	NaN	NaN	22.887	2349.9	13.170	1285.7
2250	1.0797	1.0150	1.1556	3452.9	NaN	NaN	22.875	2352.4	13.138	1284.9
2260	1.0801	1.0151	1.1571	3457.9	NaN	NaN	22.862	2354.8	13.107	1284.0
2270	1.0805	1.0152	1.1587	3462.8	NaN	NaN	22.849	2357.2	13.076	1283.1
2271	1.0805	1.0152	1.1588	3463.3	NaN	NaN	22.847	2357.4	13.073	1283.0
2280	1.0810	1.0154	1.1603	3467.7	NaN	NaN	22.835	2359.6	13.045	1282.1
2290	1.0815	1.0156	1.1620	3472.6	NaN	NaN	22.821	2362.1	13.014	1281.0
2300	1.0821	1.0158	1.1638	3477.6	NaN	NaN	22.806	2364.5	12.983	1279.9

h (km)	Y_{ax}	Y_D	Y_{SD}	T_{m0} (K)	T_{m5} (K)	T_{m10} (K)	$\log(\eta_a)$ (Pa·s)	T_{ad} (K)	α ($10^{-6}K^{-1}$)	cp (J/(kg·K))
2310	1.0827	1.0161	1.1657	3482.5	NaN	NaN	22.790	2366.9	12.953	1278.8
2320	1.0834	1.0163	1.1677	3487.5	NaN	NaN	22.774	2369.3	12.922	1277.6
2330	1.0840	1.0166	1.1695	3492.4	NaN	NaN	22.758	2371.8	12.892	1276.5
2340	1.0846	1.0169	1.1714	3497.4	NaN	NaN	22.740	2374.2	12.861	1275.4
2350	1.0853	1.0173	1.1734	3502.3	NaN	NaN	22.722	2376.6	12.831	1274.2
2360	1.0860	1.0176	1.1755	3507.3	NaN	NaN	22.703	2379.0	12.801	1273.0
2370	1.0867	1.0180	1.1777	3512.2	NaN	NaN	22.684	2381.5	12.771	1271.7
2371	1.0868	1.0180	1.1779	3512.7	NaN	NaN	22.682	2381.7	12.768	1271.5
2380	1.0875	1.0184	1.1799	3517.2	NaN	NaN	22.664	2383.9	12.741	1270.3
2390	1.0884	1.0188	1.1822	3522.2	NaN	NaN	22.643	2386.3	12.711	1268.9
2400	1.0893	1.0193	1.1846	3527.2	NaN	NaN	22.621	2388.8	12.681	1267.5
2410	1.0902	1.0198	1.1871	3532.2	NaN	NaN	22.599	2391.2	12.651	1266.0
2420	1.0912	1.0203	1.1897	3537.1	NaN	NaN	22.576	2393.6	12.622	1264.4
2430	1.0921	1.0208	1.1921	3542.1	NaN	NaN	22.552	2396.1	12.592	1263.0
2440	1.0930	1.0213	1.1946	3547.1	NaN	NaN	22.527	2398.5	12.562	1261.5
2450	1.0940	1.0219	1.1972	3552.2	NaN	NaN	22.502	2400.9	12.533	1260.0
2460	1.0950	1.0225	1.1999	3557.2	NaN	NaN	22.476	2403.4	12.503	1258.4
2470	1.0961	1.0231	1.2026	3562.2	NaN	NaN	22.449	2405.8	12.474	1256.7
2471	1.0962	1.0232	1.2029	3562.7	NaN	NaN	22.446	2406.1	12.471	1256.6
2480	1.0972	1.0238	1.2055	3567.3	NaN	NaN	22.421	2408.3	12.444	1255.0
2490	1.0984	1.0244	1.2084	3572.3	NaN	NaN	22.392	2410.7	12.415	1253.3
2500	1.0996	1.0251	1.2114	3577.4	NaN	NaN	22.362	2413.1	12.385	1251.5
2510	1.1009	1.0258	1.2145	3582.4	NaN	NaN	22.331	2415.6	12.356	1249.6
2520	1.1022	1.0266	1.2177	3587.5	NaN	NaN	22.300	2418.1	12.326	1247.6
2530	1.1034	1.0273	1.2207	3592.6	NaN	NaN	22.267	2420.5	12.297	1245.8
2540	1.1047	1.0281	1.2238	3597.6	NaN	NaN	22.234	2423.0	12.267	1244.0
2550	1.1060	1.0289	1.2269	3602.8	NaN	NaN	22.200	2425.4	12.238	1242.1
2560	1.1073	1.0297	1.2302	3607.9	NaN	NaN	22.164	2427.9	12.208	1240.1
2570	1.1087	1.0306	1.2335	3613.0	NaN	NaN	22.128	2430.3	12.179	1238.1
2571	1.1088	1.0307	1.2339	3613.5	NaN	NaN	22.124	2430.6	12.176	1237.9
2580	1.1101	1.0315	1.2370	3618.1	NaN	NaN	22.090	2432.8	12.149	1236.0
2590	1.1116	1.0324	1.2405	3623.2	NaN	NaN	22.052	2435.3	12.120	1233.9
2600	1.1132	1.0333	1.2441	3628.4	NaN	NaN	22.012	2437.8	12.090	1231.7
2610	1.1148	1.0342	1.2478	3633.6	NaN	NaN	21.972	2440.2	12.061	1229.4
2620	1.1165	1.0352	1.2516	3638.8	NaN	NaN	21.930	2442.7	12.031	1227.1
2630	1.1180	1.0362	1.2553	3643.9	NaN	NaN	21.887	2445.2	12.001	1224.9
2640	1.1195	1.0372	1.2589	3649.1	NaN	NaN	21.843	2447.7	11.972	1222.7
2650	1.1212	1.0382	1.2627	3654.3	NaN	NaN	21.798	2450.2	11.942	1220.4
2660	1.1228	1.0393	1.2665	3659.6	NaN	NaN	21.752	2452.6	11.912	1218.0
2670	1.1246	1.0404	1.2705	3664.8	NaN	NaN	21.704	2455.1	11.882	1215.6
2671	1.1247	1.0405	1.2709	3665.3	NaN	NaN	21.699	2455.4	11.879	1215.4
2680	1.1263	1.0415	1.2745	3670.1	NaN	NaN	21.655	2457.6	11.852	1213.1
2690	1.1282	1.0426	1.2787	3675.3	NaN	NaN	21.605	2460.1	11.822	1210.6
2700	1.1301	1.0438	1.2829	3680.6	NaN	NaN	21.554	2462.6	11.792	1208.0
2710	1.1320	1.0449	1.2872	3685.9	NaN	NaN	21.501	2465.2	11.761	1205.3
2720	1.1340	1.0461	1.2916	3691.2	NaN	NaN	21.447	2467.7	11.731	1202.6
2730	1.1360	1.0474	1.2961	3696.5	NaN	NaN	21.392	2470.2	11.701	1199.8
2740	1.1381	1.0486	1.3007	3701.9	NaN	NaN	21.336	2472.7	11.670	1197.0
2741	1.1384	1.0487	1.3012	3702.4	NaN	NaN	21.330	2473.0	11.667	1196.7
2741	1.1384	0.3365	0.2547	3702.4	NaN	NaN	21.330	2473.0	11.667	1196.7
2750	1.1406	0.3362	0.2549	3707.2	NaN	NaN	21.278	2475.2	11.644	1192.6
2760	1.1427	0.3360	0.2551	3712.6	NaN	NaN	21.218	2477.8	11.618	1188.4
2770	1.1445	0.3357	0.2554	3718.1	NaN	NaN	21.157	2480.3	11.593	1184.6
2771	1.1447	0.3357	0.2554	3718.6	NaN	NaN	21.151	2480.6	11.590	1184.2
2780	1.1460	0.3354	0.2557	3723.5	NaN	NaN	21.095	2482.9	11.567	1181.1
2790	1.1472	0.3351	0.2560	3728.9	NaN	NaN	21.031	2485.5	11.542	1178.0
2800	1.1481	0.3349	0.2564	3734.4	NaN	NaN	20.966	2488.0	11.516	1175.2
2810	1.1486	0.3346	0.2568	3739.9	NaN	NaN	20.900	2490.6	11.491	1172.7
2820	1.1488	0.3343	0.2572	3745.4	NaN	NaN	20.831	2493.2	11.466	1170.6
2830	1.1488	0.3340	0.2572	3750.9	NaN	NaN	20.761	2495.8	11.441	1168.8
2840	1.1483	0.3337	0.2572	3756.4	NaN	NaN	20.690	2498.4	11.416	1167.4
2850	1.1476	0.3334	0.2572	3762.0	NaN	NaN	20.617	2501.0	11.391	1166.3
2860	1.1465	0.3331	0.2573	3767.5	NaN	NaN	20.542	2503.6	11.366	1165.5
2870	1.1451	0.3328	0.2574	3773.1	NaN	NaN	20.466	2506.2	11.342	1165.0

h(km)	γ_{ax}	γ_D	γ_{SD}	T_{m0} (K)	T_{m5} (K)	T_{m10} (K)	$\log(\eta_4)$ (Pa·s)	T_{ad} (K)	α ($10^{-6}K^{-1}$)	c_p (J/(kg·K))
2871	1.1450	0.3328	0.2574	3773.6	NaN	NaN	20.458	2506.4	11.339	1165.0
2880	1.1434	0.3325	0.2575	3778.6	NaN	NaN	20.388	2508.8	11.317	1164.9
2885	1.1425	0.3324	0.2575	3781.4	NaN	NaN	20.348	2510.1	11.305	1165.0
2890	1.1414	0.3322	0.2576	3784.2	NaN	NaN	20.308	2511.4	11.292	1165.2
2891	1.1412	0.3322	0.2576	3784.8	NaN	NaN	20.300	2511.6	11.290	1165.2

Table B2. Model parameters

Parameter	Description	Value	Dimension
r_{min}	Inner radius of spherical shell	3.480×10^6	m
r_{max}	Outer radius of spherical shell	6.371×10^6	m
	Temperature at the shell boundary	288	K
h_1	Depth of the exothermic phase boundary	4.10×10^5	m
h_2	Depth of the endothermic phase boundary	6.60×10^5	m
γ_1	Clausius–Clapeyron slope for the olivine–wadsleyite transition	$+1.6 \times 10^6$	$\text{Pa}\cdot\text{K}^{-1}$
γ_2	Clausius–Clapeyron slope for the ringwoodite–perovskite transition	-2.5×10^6	$\text{Pa}\cdot\text{K}^{-1}$
f_{a1}	Non-dimensional density jump for the olivine–wadsleyite transition	0.0547	
f_{a2}	Non-dimensional density jump for the ringwoodite–perovskite transition	0.0848	
	Begin of the thermal evolution of the <i>solid</i> Earth’s silicate mantle	4.490×10^9	a
d_1	Non-dimensional transition width for the olivine–wadsleyite transition	0.05	
d_2	Non-dimensional transition width for the ringwoodite–perovskite transition	0.05	
	Begin of the radioactive decay	4.565×10^9	a
c_t	Factor of the lateral viscosity variation	1	
k	Thermal conductivity	5	$\text{W}\cdot\text{m}^{-1}\cdot\text{K}^{-1}$
$nr + 1$	Number of radial levels	33	
	Number of gridpoints	1.351746×10^6	

156 **References**

157 **References**

158 Christensen, U.R., Yuen, D.A., 1985. Layered convection induced by phase
159 transitions. *Journal of Geophysical Research* 90, 10291–10300.

160 Dziewonski, A.M., Anderson, D.L., 1981. Preliminary reference Earth model.
161 *Physics of the Earth and Planetary Interiors* 25, 297–356.

162 Litasov, K.D., 2011. Physicochemical conditions for melting in the Earth's
163 mantle containing a C-O-H fluid (from experimental data). *Russian Geol-
164 ogy and Geophysics* 52, 475–492.

165 Mitrovica, J.X., Forte, A.M., 2004. A new inference of mantle viscosity based
166 upon joint inversion of convection and glacial isostatic adjustment data.
167 *Earth Planet. Sci. Lett.* 225 (1), 177–189.

168 Richter, F.M., 1973. Finite amplitude convection through a phase boundary.
169 *Geophysical Journal of the Royal Astronomical Society* 35, 265–276.

170 Stacey, F.D., Davis, P.M., 2009. *Physics of the Earth*. 4th ed., Cambridge
171 University Press, Cambridge, UK.